JOURNAL OF AGRICULTURAL AND FOOD CHEMISTRY

Article

pubs.acs.org/JAFC

Development of Metal−Organic Framework for Gaseous Plant Hormone Encapsulation To Manage Ripening of Climacteric Produce

Boce Zhang,[†,‡] Yaguang Luo,[*,†,‡] Kelsey Kanyuck,[§] Gary Bauchan,[∥] Joseph Mowery,[∥] and Peter Zavalij[⊥]

[†]Environmental Microbial and Food Safety Laboratory, Agricultural Research Service, [‡]Food Quality Laboratory, Agricultural Research Service, and [∥]Electron and Confocal Microscope Unit, Agricultural Research Service, United States Department of Agriculture, Beltsville, Maryland 20705, United States

[§]Department of Nutrition and Food Science, and [⊥]Department of Chemistry and Biochemistry, University of Maryland, College Park, Maryland 20742, United States

ABSTRACT: Controlled ripening of climacteric fruits, such as bananas and avocados, is a critical step to provide consumers with high-quality products while reducing postharvest losses. Prior to ripening, these fruits can be stored for an extended period of time but are usually not suitable for consumption. However, once ripening is initiated, they undergo irreversible changes that lead to rapid quality loss and decay if not consumed within a short window of time. Therefore, technologies to slow the ripening process after its onset or to stimulate ripening immediately before consumption are in high demand. In this study, we developed a solid porous metal−organic framework (MOF) to encapsulate gaseous ethylene for subsequent release. We evaluated the feasibility of this technology for on-demand stimulated ripening of bananas and avocados. Copper terephthalate (CuTPA) MOF was synthesized via a solvothermal method and loaded with ethylene gas. Its crystalline structure and chemical composition were characterized by X-ray diffraction crystallography, porosity by N_2 and ethylene isotherms, and morphology by electron microscopy. The MOF loaded with ethylene (MOF−ethylene) was placed inside sealed containers with preclimacteric bananas and avocados and stored at 16 °C. The headspace gas composition and fruit color and texture were monitored periodically. Results showed that this CuTPA MOF is highly porous, with a total pore volume of 0.39 cm^3/g. A 50 mg portion of MOF−ethylene can absorb and release up to 654 μL/L of ethylene in a 4 L container. MOF−ethylene significantly accelerated the ripening-related color and firmness changes of treated bananas and avocados. This result suggests that MOF−ethylene technology could be used for postharvest application to stimulate ripening just before the point of consumption.

KEYWORDS: *metal−organic framework, ethylene, climacteric produce, food waste*

1. INTRODUCTION

Spoilage of fruits and vegetables accounts for 50% of the total food waste.[1] Among these losses, 78% is generated at the retail and household stages of the food supply chain. Climacteric fruits can be picked at the preclimacteric stage and stored for extended periods of time prior to ripening. Ethylene exposure is frequently used to stimulate commercial ripening, so that fruits can be prepared for consumption. After ripening is initiated, ethylene is produced by an autocatalytic biosynthesis. This metabolic activity causes fruits to rapidly and irreversibly deteriorate once past their optimal ripeness stage, which often results in significant loss and waste if the products cannot be consumed immediately.

Measuring and manipulating the amount of the plant hormone ethylene applied exogenously is the key to predicting and inducing the ripening and flavor development of climacteric fruits. The gaseous plant hormone ethylene acts at trace levels to influence many aspects of plant development and response to the environment, such as flower opening, senescence, leaf abscission, adventitious root initiation, seed dormancy, and ripening of climacteric fruits.[2,3] Ethylene is considered to be generally recognized as safe for the treatment of produce by the United States Food and Drug Administration and has broad applications in both pre- and postharvest stages. Ethylene gas has been widely used commercially to stimulate and induce the ripening of bananas, avocados, tomatoes, and mangos and for the degreening of citrus.[4−7] However, ethylene is highly flammable and combustible at concentrations above 27 000 μL/L and, therefore, requires special care during shipping, storage, and application.[4−6] The most common source of ethylene gas is catalytically generated during the incomplete combustion of alcohols, such as ethanol and isopropanol, or organic fuels, such as propane and natural gas, both of which require on-site maintenance of flammable materials.[4,8−13]

An alternative to ethylene gas is the artificial ripening agent ethephon or 2-chloroethylphosphonic acid.[10,14] Registered as a pesticide, ethephon is approved for preharvest application on tomatoes and table grapes with a maximum residue limit of 2 μL/L. It is often applied by direct spray or dipping of the ethephon solutions on produce surfaces.[15−17] Natural degradation generates ethylene when ethephon reaches the internal plant tissues.[17,18] Ethephon is not approved for postharvest application via direct spray or dipping, but its indirect use for postharvest treatment via the generation of ethylene gas is permitted.[15−17] However, both ethephon and sodium hydroxide (NaOH) pellets required to liberate ethylene from ethephon are corrosive and not suitable for consumer and retail store applications.[15−17] Additionally, reports have shown that the application of ethephon can trigger heterogeneous ripening and rotting, which reduces the

Received: May 6, 2016
Accepted: June 2, 2016
Published: June 2, 2016

DOI: 10.1021/acs.jafc.6b02072
J. Agric. Food Chem. 2016, 64, 5164−5170

shelf life and market value of the produce.[19] Thus, a method to directly apply ethylene without safety hazard is highly desired. One potential approach could be to induce and promote ripening with small application volumes near the consumer end of the food supply chain.

A novel approach to the safe handling of hazardous gaseous materials is the encapsulation and release of these gases using a solid porous material. Zeolite was the first porous ethylene absorbent developed almost 2 decades ago.[20−24] Natural zeolite, potassium-permanganate-impregnated zeolite, and zeolite-qenhanced films or paper carton liners are currently being marketed for ethylene adsorption with horticultural commodities.[25] However, although zeolite-based materials are well-studied as ethylene absorbers and neutralizers, there have been no reports about the application of zeolite for ethylene encapsulation and release. Furthermore, the small pore size (3−8 Å) of the zeolite materials represents a major limitation for exchange and release of gaseous molecules.[26]

Metal−organic framework (MOF) is a new class of engineered materials with unique physical−chemical properties that have been used for the encapsulation of combustible gases. The crystalline structures of MOF are highly porous as a result of their one-, two-, and three-dimensional extended polymeric structures formed by coordination bonds between metal atoms and organic ligands.[27−29] Numerous MOF materials have been developed with a large variety of functionalities and applications by adjusting ligand property, metal atom, spacer length, and synthesis conditions.[27−29] Recently, the cost of manufacturing MOF materials has been significantly reduced and is now comparable to the zeolite-based materials. Currently, the commercial use of MOF is primarily limited to clean-energy-related applications, while food and agricultural applications are extremely rare. This is the first report of the development and application of a MOF to encapsulate and release ethylene for the stimulation of ripening in climacteric produce.

2. EXPERIMENTAL SECTION

2.1. Materials and Chemicals. Copper(II) acetate (CuAc), terephthalic acid (TPA), dimethylformamide (DMF), methanol, and ethanol were purchased from Sigma-Aldrich (St. Louis, MO). Mature preclimacteric "Hass" avocados (*Persea americana*) were directly purchased from a local produce distribution center (Coastal Sunbelt, Savage, MD). Mature green, preclimacteric Cavendish-type bananas (*Musa acuminata*) that had been pretreated with ethylene the previous day were purchased from a local supermarket (Shoppers Food and Pharmacy, College Park, MD) on the day of experimentation.

2.2. Solvothermal Synthesis of Copper Terephthalate (CuTPA). The CuTPA MOF was synthesized via a solvothermal method, using a modified version of Carson's method (eq 1).[28] A mixture of reagents was prepared by dissolving 74 mg of CuAc and 92 mg of TPA in a solvent system of 10 mL of DMF and 10 mL of methanol inside a Teflon-lined autoclave reactor. The solution was then sonicated for 5 min to dissolve all particles and incubated for 24 h at room temperature. The MOF product was synthesized by heating the reactor to 120 °C for 24 h. The crystalline, blue solids were centrifuged and washed 3 times with ethanol. The product was then transferred to a 5 mL glass beaker, dried, and activated in a vacuum oven at 170 °C.

$$\mathrm{Cu(CH_3COO)_2} + \mathrm{C_6H_4(COOH)_2} \times \xrightarrow[\text{autoclave, 120°C}]{\text{DMF/MeOH}} \mathrm{Cu[C_6H_4(COO)_2](DMF)} + 2\mathrm{CH_3COOH} \quad (1)$$

2.3. X-ray Diffraction (XRD) Crystallography. XRD was used to characterize the crystal structure and chemical composition of CuTPA. Samples were prepared according to our previous reports.[30] Sample powders were attached to specimen holders by double-sided tape. Powder diffraction was acquired using a powder diffractometer (Bruker D8 Advance, Billerica, MA) equipped with a Ni β-filter, a sealed Cu Kα tube (wavelength of 1.5406 Å), and a position sensitive LynxEye detector. The diffractometer was operated in Bragg−Brentano mode (θ−θ geometry). Spectrum analysis and phase identification were performed using the International Center for Diffraction Data (ICDD) powder diffraction database.

2.4. Characterization of MOF Morphology. Scanning electron micrographs were captured using S-4700 low-temperature field emission scanning electron microscopy (LT-SEM, Hitachi High Technologies America, Inc., Pleasanton, CA) with a Quorum Cryo-Prep Chamber (Quorum Technologies, East Sussex, U.K.). All MOF samples were coated with a thin layer of Pt nanoparticle using a sputter coater. All images were captured at 10 kV accelerating voltage and a 10 mm working distance with a 4pi Analysis system (Durham, NC).

In preparation for transmission electron microscopy (TEM), solutions of MOF in ethanol were applied directly to 400-mesh carbon-coated copper grids and allowed to absorb for 30 min. Excess solution was wicked off, and grids were air-dried. Grids were imaged at 80 kV with Hitachi HT-7700 TEM (Hitachi, Tokyo, Japan).

2.5. Characterization of MOF Porosity. N_2 isotherms were measured on a Micromeritics TriStar II Plus (Norcross, GA) unit to full saturation [i.e., a relative pressure (P/P_0, where P_0 equals 101.3 kPa) of approximately 1.0 at 77 K] to enable Brunauer−Emmett−Teller (BET) surface area and total pore volume (TOPV) analyses to be performed. In addition, a low pressure (P < 101.3 kPa) ethylene isotherm was measured on a Micromeritics ASAP unit at 25 °C. The samples were activated on a Smart VacPrep (Micromeritics, Norcross, GA) unit by degassing in stages up to 150 °C with a series of ramp/soak steps under dynamic vacuum. The sample preparation was performed by drawing a vacuum at ambient temperature, raising the temperature 1 °C/min to 80 °C, holding at 80 °C until a vacuum level of <0.133 Pa was achieved, and then holding the sample at 80 °C for an additional 1 h. The temperature was then ramped at 10 °C/min to a series of preset temperatures following the same protocol (i.e., maintaining the set temperature until a vacuum level of <0.133 Pa was attained) and then holding the sample at the set temperature for an additional 1 h. The preset temperatures used were 100, 120, and 150 °C. The sample was held at the final temperature until a vacuum level of <0.0133 Pa was achieved. The cumulative volume was calculated on the basis of a Barrett−Joyner−Halenda (BJH) analysis, which relates the pore size to the relative pressure.

2.6. Loading MOF with Ethylene. After activation in a vacuum oven, a 2 mL capsule filled with MOF was transferred to a preparation chamber, loaded (infused) with ethylene by applying a vacuum to the chamber for 30 min, and then feeding pure ethylene gas into the chamber until reaching ambient pressure (120 min). The vacuum and purge process allowed for high exchange and encapsulation efficiency of ethylene inside the MOF pores.

2.7. Application of MOF Loaded with Ethylene (MOF−Ethylene) for Fruit Ripening. The ripening experiment was designed to simulate the application of continuous exogenous ethylene via MOF−ethylene to a small volume of climacteric produce near the consumer end of the food supply chain. MOF−ethylene was placed at the bottom of eight 4 L airtight produce containers. Four green bananas or four unripened avocados were placed in each of the eight containers with MOF−ethylene and in an additional 16 containers without. Eight of the additional containers were treated with 1000 μL/L of ethylene gas, while the other eight were controls containing air without ethylene. Equal numbers of avocados and bananas were exposed to each treatment, and all containers were maintained at 16 °C.

Ethylene levels in the container were measured using a gas chromatograph (HP 5890A, Hewlett-Packard, Golden, CO) equipped with a packed Haysep Q column (1.2 m × 3 mm, 60:80 mesh), a Shimadzu C-R5A Chromatopac Integrator, and a flame ionization detector (FID). The inlet line pressures of carrier gas (He), air, and hydrogen were 20, 40, and 30 psi, respectively, and the FID flow rates were 30, 60, and 45 mL/min, respectively. The detector, oven (column), and injector were operated at 250, 70, and 200 °C, respectively,

DOI: 10.1021/acs.jafc.6b02072
J. Agric. Food Chem. 2016, 64, 5164−5170

according to our previous report.[31] Ethylene levels were expressed in units of microliters per liter after comparison to a 1000 μL/L ethylene standard (Air Liquide America Specialty Gases, Houston, TX).

2.8. Quality Evaluation of Fruits Treated with MOF−Ethylene. The O_2 and CO_2 concentrations within the containers were measured using a gas analyzer system (Gaspace Advance GS3Micro, Illinois Instrument, Johnsbury, IL).[32] The analyzer takes 2.5 mL of the headspace to give an accurate and stable reading at the flow rate of 0.17 mL/s. Each measurement was conducted in parallel with four containers per treatment, each containing four fruit, and the measurements were repeated at least 3 times.

The color change of the produce was measured using a Minolta colorimeter (Minolta Co., Ltd., Japan), which measures the color-opponent space of L^*, a^*, and b^* values.[9] The values reported are the mean of three readings analyzed equidistant from stem and blossom ends of the surface skin of each of the bananas or two readings from the equatorial region on the surface of each avocado.[8] Similarly, the color measurement was conducted with four replications per treatment and four bananas per replication, and each measurement was repeated 3 times. For bananas, the letter '*a*' is an indicator of green, with a higher '*a*' value indicating less intense green; the letter '*b*' is an indicator of yellow, with a higher '*b*' value indicating more intense yellow. For avocados, the degree of browning is expressed by the percent decrease in the L value and is calculated by subtracting the L value of samples from the time zero L value and dividing by the time zero value.

The firmness was measured using a texture analyzer (TA.XT plus, Stable Micro System, Surrey, U.K.). Banana and avocado samples were peeled and stabilized on the platform using modeling clay before making each penetration measurement. Banana pulp was measured in three locations: toward the stem end, middle, and blossom end, while avocados were measured at three sites around the equatorial region.[8] The texture analysis was conducted on four fruit per container and four containers per treatment. The textural property was measured as the resistance in newtons of the fruit pulp to penetration by a cylindrical probe with the diameter of 11.0 mm. The penetration rate was 0.5 mm/s, and the penetration distance was 10.0 mm. The firmness was measured as the slope of resistance and penetration distance at the initial linear region before destruction of the pulp tissue.

2.9. Statistical Analysis. The experiment was repeated 3 times with four replications per treatment for each trial. Statistical analysis was conducted using SAS software (version 9.2, SAS Institute, Inc., Cary, NC). Analysis of variance (ANOVA), Tukey's multiple comparison tests, and Dunnett's tests were performed with a p value set at 0.05.

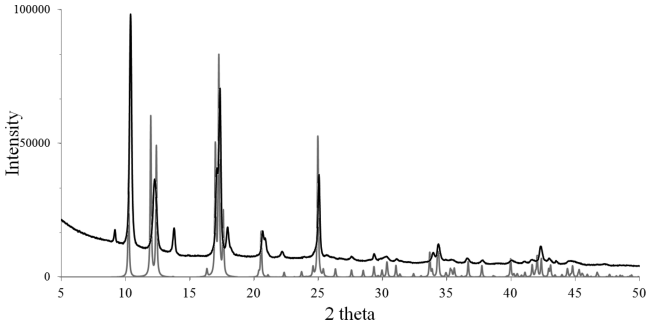

Figure 1. Comparison of (top) XRD patterns for our laboratory-produced CuTPA MOF powders and (bottom) identified single-crystal diffraction pattern for CuTPA from the ICDD database.

3. RESULTS AND DISCUSSION

3.1. MOF Synthesis and Characterization. *3.1.1. XRD.* The solvothermal synthesis of CuTPA resulted in a blue powder of mixed MOF crystals.[28] Sealed autoclave reactors with Teflon liners were used in the solvothermal synthesis of CuTPA to create a high-pressure methanol vapor-filled environment. These conditions facilitated the high-quality crystal growth by forcing the dissolution of the DMF base and the deprotonation of TPA.[28]

The XRD analysis was carried out to verify the crystal structure. The powder diffraction patterns (Figure 1) can be identified because they nearly match the previously reported single-crystal CuTPA from the ICDD database.[28] The peak intensity of CuTPA powder at 12.2°, depicted as the (201) plane, was slightly lower than that of its single crystal. This result could be attributable to the anisotropic property of the powder diffraction. Figure 2a shows the crystalline structure of powder CuTPA. In the complex, TPA ligands form bidentate coordination bonds with the Cu^{II} dimer, and each Cu^{II} atom is also linked to a DMF molecule. The structure is similar to the previously reported zinc terephthalate (MOF-2).[29] Figure 2b shows a hypothetical schematic of the channels and pores inside the CuTPA crystals, which are formed between layers of the laminated structures that are covalently bonded to the (001) plane.

3.1.2. Electron Microscopy. Figure 3a shows the TEM micrograph of the CuTPA powder. The particles appear rectangular cuboid in shape with a diameter of about 187 ± 32 nm. The SEM micrograph (Figure 3b) shows similar morphology and particle size. Besides the internal pores of the MOF crystals, the gaps (e.g., cavities and crevices) between closely packed CuTPA MOF particles can also contribute to the storage and release of ethylene.

3.1.3. Porosity and Ethylene Encapsulation Capacity. The porosity measurement is a characterization of storage efficacy and capacity of CuTPA MOF for gaseous materials. The N_2 isotherms (Figure 4a) evaluate the total capacity and the composition of empty crevices as micropores (<2 nm), mesopores (between 2 and 50 nm), and macropores (>50 nm). In this study,

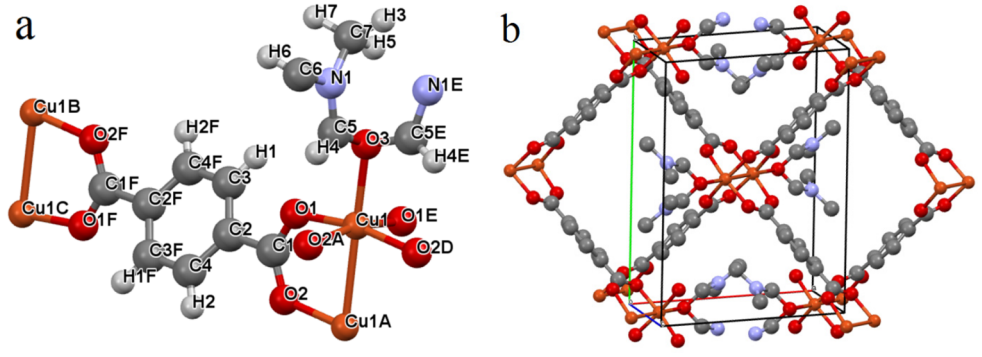

Figure 2. (a) Molecular structure of the CuTPA MOF and (b) hypothetical view of a CuTPA unit cell, comprising eight molecules, with associated channels that provide the high surface area and porosity for ethylene encapsulation.

DOI: 10.1021/acs.jafc.6b02072
J. Agric. Food Chem. 2016, 64, 5164−5170

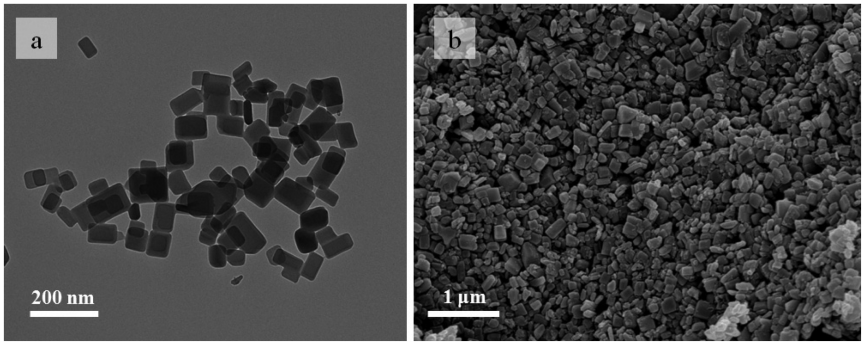

Figure 3. (a) Micrograph of CuTPA powder from TEM and (b) micrograph of CuTPA powder from SEM.

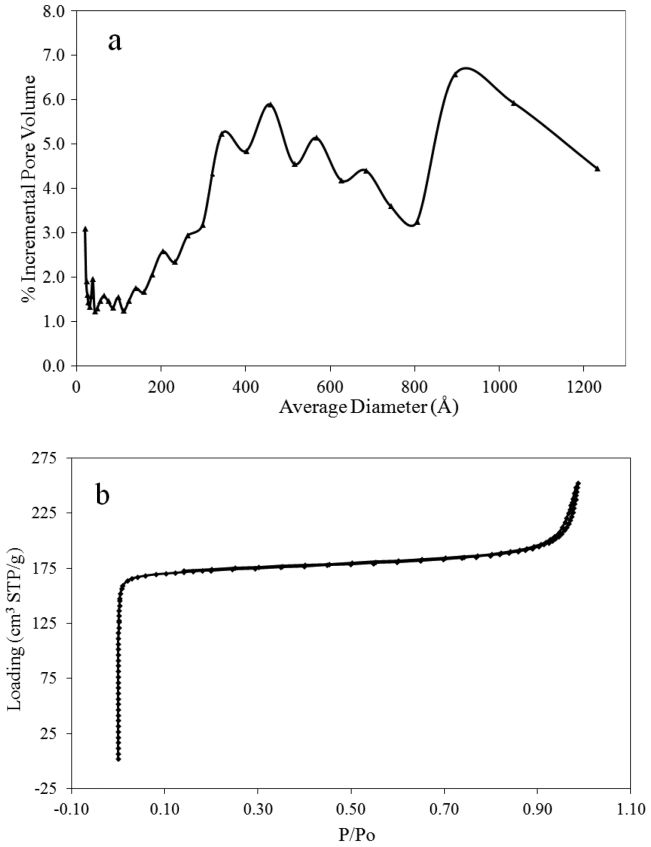

Figure 4. (a) Cumulative (dashed line) and percentage incremental (solid line) pore size (Å) distribution from desorption measured at 77 K and (b) N_2 adsorption−desorption isotherms measured at 77 K as a function of the relative pressure (P/P_0). The error bar was not included in this graph, because the standard error was less than <0.6%.

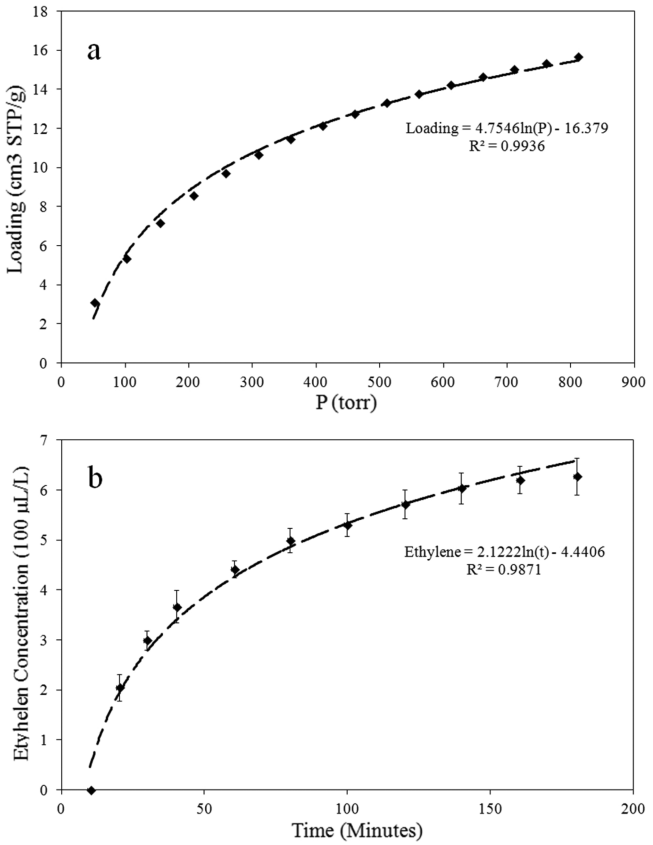

Figure 5. (a) Ethylene isotherm measured at standard temperature and pressure (STP, 273.15 K and 0.1 MPa) for sample CuTPA. The error bar was not included in this graph, because the standard error was less than <0.6%. (b) Ethylene release kinetics from 50 mg of MOF−ethylene in a 4 L container.

N_2 isotherms reveal a relatively high BET surface area for CuTPA of 708 m^2/g. The total pore volume is 0.39 cm^3/g, and the micropore volume is 0.246 m^3/g. The majority of the pores are micropores (<2 nm) and represent approximately 63% of the total pore volume (Figure 4a), which is consistent with previous reports.[28,29]

The hysteresis loop (Figure 4b) indicates the recovery of gaseous materials by comparing adsorption and release isotherms. The lack of significant hysteresis for CuTPA MOF suggests that the absorbed gaseous materials can achieve a very high recovery rate upon release under vacuum conditions.

The ethylene isotherm and release kinetics (Figure 5) indicate the capacity of the CuTPA MOF to adsorb and release ethylene. The ethylene isotherm at 25 °C is presented in Figure 5a. Figure 5b shows the release kinetics of ethylene from 50 mg of MOF−ethylene into a 4 L container. The release kinetics fit a logarithmic model, which indicates that the release rate was highest when the MOF−ethylene was first placed into a new container filled with air. The decrease in the release rate over time could be attributed to the depletion of ethylene stored in the MOF−ethylene. Upon the loading of MOF with ethylene at ambient temperature and pressure according to the method described earlier, a total of 654 μL of ethylene was absorbed into the internal pores and external gaps in the 50 mg portion of MOF−ethylene. In the release kinetic study, 627 μL of ethylene was released into the container after 180 min, which accounted for 95.8% of total

DOI: 10.1021/acs.jafc.6b02072
J. Agric. Food Chem. 2016, 64, 5164−5170

absorbed ethylene in MOF−ethylene. An appropriate packaging system that can stabilize ethylene encapsulation within the MOF−ethylene needs further investigation before practical application.

3.2. Induced Ripening of Climacteric Produce. Prior to this study, a preliminary experiment was conducted using untreated green bananas purchased from the same distribution center as the avocados. The results of this preliminary study followed the same trends as the current study with somewhat longer ripening times for all treatments: 1000 μL/L of ethylene standard, MOF−ethylene, and control (air without ethylene). On the basis of visual observations and texture data, the MOF−ethylene treatment was effective in the accelerated ripening of bananas previously untreated with ethylene.

3.2.1. Induced Ripening of Bananas. The effectiveness of the CuTPA MOF as a solid matrix for ethylene encapsulation and release was investigated. Figure 6a shows the colorimetric analyses

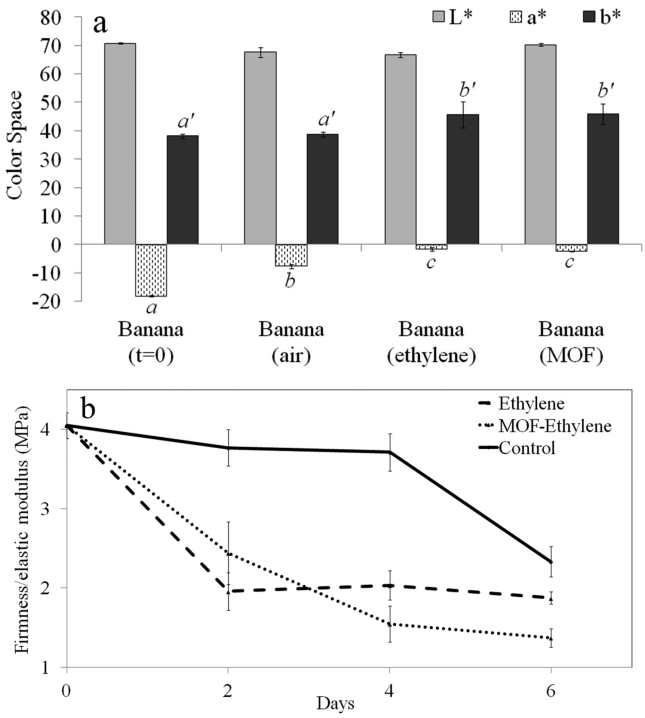

Figure 6. (a) Color and (b) firmness changes of bananas after 48 h of ethylene treatment and an additional 48 h of storage. 't = 0' represents the start of the continuous exogenous ethylene treatment, which was 24 h after the pretreatment at a local distribution facility. Means marked with different letters indicated the significant difference between each other upon ANOVA Tukey's test ($p < 0.05$).

of banana surfaces. Banana samples treated with 1000 μL/L of ethylene or MOF−ethylene showed a significant decrease in green (higher a^* value) and increase in yellow (higher b^* value), while the control remained unchanged in comparison to the measurement before ripening treatment (t = 0). The decrease in the a^* value and increase in the b^* value compared to the preclimacteric control indicate that treatment of bananas with 1000 μL/L of ethylene or MOF−ethylene significantly accelerated the ripening process.

The textural properties of bananas (shown in Figure 6b) were significantly different between the ethylene-treated samples and the preclimacteric controls. The firmness measurements indicate that bananas became softer after 2 days of ethylene and MOF−ethylene treatments. The MOF−ethylene treatment decreased the firmness of the banana by 39.8% in 2 days (Figure 6b) and was not significantly different from the ethylene treatment. The firmness of the control bananas only decreased by 7.0% during the same time period. These results are consistent with previous reports.[11,12,33]

The gas composition of the sealed container (ethylene, oxygen, and carbon dioxide) was monitored during the ripening of bananas. Figure 8 shows the change in the ethylene concentration in a 4 L jar after 2 days of ripening. The ethylene concentration in the container with only MOF−ethylene (50 mg) reached 654 μL/L, while the empty control container had no ethylene (Figure 8). The ethylene concentration in the container with banana and MOF−ethylene reached 347 μL/L. The absorption of ethylene by the bananas suggests that the MOF−ethylene treatment accelerated the fruit's synthesis of ethylene and the ripening process. The rapid accumulation of CO_2 in the treatment jars with MOF−ethylene also indicates an accelerated ripening process stimulated by exogenous ethylene (Figure 9).

3.2.2. Induced Ripening of Avocados. Avocado skin color darkened slightly after ethylene and MOF−ethylene treatment for 2 days (Figure 7a), and the fruits became softer after

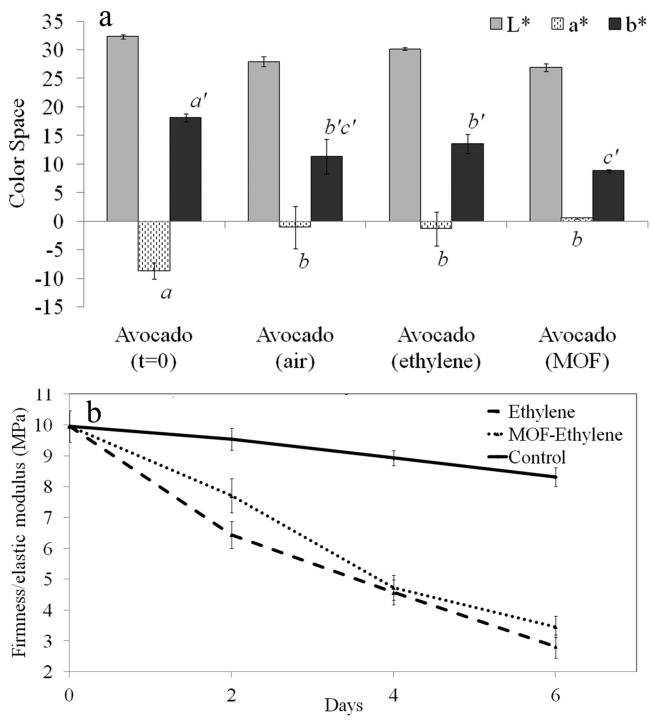

Figure 7. (a) Color and (b) firmness changes of avocados after 48 h of ethylene treatment and an additional 96 h of storage. Means marked with different letters indicated the significant difference between each other upon ANOVA Tukey's test ($p < 0.05$).

4 additional days of storage (Figure 7b). The avocados treated with MOF−ethylene softened by 65%, which was not significantly different from the 71% decrease in firmness observed in the ethylene-treated control. The untreated avocados only lost 16% of the initial firmness after the 6 day storage period (Figure 7b), which is also consistent with previous reports.[34]

Similarly, Figure 8 shows the change in the ethylene concentration in the container during avocado ripening. The ethylene- and MOF−ethylene-treated samples had significantly higher accumulation of the ethylene concentration during ripening compared to the controls without exogenous ethylene. The avocado absorbed

DOI: 10.1021/acs.jafc.6b02072
J. Agric. Food Chem. 2016, 64, 5164−5170

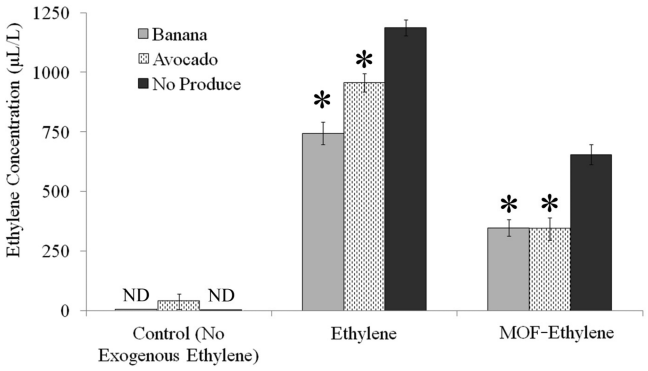

Figure 8. Changes of the ethylene concentration after 48 h in 4 L containers with banana and avocado, continuously treated with air, exogenous 1000 μL/L of ethylene, or 50 mg of MOF−ethylene. Means marked with asterisks indicated the significant difference between the control and no produce samples from ANOVA Dunnett's test ($p < 0.05$). "ND" indicates not detected in the figure.

the gaseous ethylene, which stimulated the ripening process. This metabolic process was also confirmed by the change of O_2 and CO_2 composition during the ripening process. When the ripening process was stimulated, the avocado generated more cumulative CO_2 in the container (Figure 9).

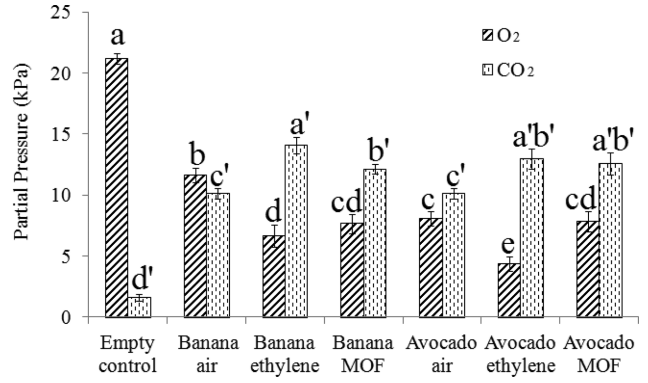

Figure 9. Changes in gas composition over 48 h of continuous 1000 μL/L of ethylene and MOF−ethylene treatment. Means marked with different letters indicated the significant difference between each other upon ANOVA Tukey's test ($p < 0.05$).

Sealed containers were used in this study to measure accumulated ethylene release. Bananas and avocados are living plant organs and, therefore, respire, which resulted in high levels (near 15%) of CO_2 in several containers. In containers with high CO_2 levels, tissue injury and ethanol-based off-odors were noted. Therefore, packages with an O_2 and CO_2 transmission rate similar to the O_2 consumption and CO_2 production rates of the fruits may be a better method for storing produce during treatment, as long as the ethylene transmission is negligible.

While this study demonstrated the effectiveness of this technology for ripening control, additional studies are needed to optimize treatment conditions in the future. Further research beyond this study may include (1) development of a proper packaging system to stabilize ethylene encapsulation in the MOF material, (2) optimization of the MOF−ethylene treatment to maximize food quality and safety outcomes, (3) enhancement of the MOF molecular design to improve encapsulation capacity and stability in a high-moisture environment, which is often present in food and agricultural applications.

In summary, a porous CuTPA MOF was synthesized and characterized. The function of MOF to encapsulate and release gaseous plant hormone, ethylene, for fruit ripening was further explored. The CuTPA MOF material has a total pore volume of 0.39 cm^3/g. In a 4 L container, a 50 mg portion of the substance can absorb and release up to 654 μL/L of ethylene, which creates an atmosphere enriched with sufficient ethylene to stimulate fruit ripening but also maintains the level below the safety allowance of 27 000 μL/L.

Previously untreated avocados and ethylene-pretreated green bananas were used in this study. MOF−ethylene treatment accelerated the ripening process of both fruits by reducing tissue firmness and facilitating the ripening-related color change. This suggests that MOF−ethylene can be used not only to treat preclimacteric fruits to stimulate ripening but also to further shorten the ripening time for those that previously received ethylene treatment. This MOF−ethylene technology could offer consumers and other handlers an option to treat climacteric fruits at the end of the supply chain, making high-quality ripe fruit available as needed while minimizing postharvest losses.

AUTHOR INFORMATION

Corresponding Author

*Telephone: 001-301-504-6186. Fax: 001-301-504-5107. E-mail: yaguang.luo@ars.usda.gov.

Notes

The authors declare the following competing financial interest(s): The invention reported in this paper has been documented and sought for U.S. patent protection (14/861,086). For more information, please contact The Office of Technology Transfer (OTT), USDA.

ACKNOWLEDGMENTS

This work was supported by USDA-NIFA Specialty Crop Research Initiative Grant Award No. MDW-2010-01165. The authors acknowledge the support of Dr. John Zielinski at Intertek Chemicals and Pharmaceuticals service to conduct the work of N_2/ethylene isotherms, BET, and TOPV measurements. The mention of trade names or commercial products in this publication is solely for the purpose of providing specific information and does not imply recommendation or endorsement by the United States Department of Agriculture (USDA). The USDA is an equal opportunity provider and employer.

REFERENCES

(1) Blanke, M. Reducing ethylene levels along the food supply chain: A key to reducing food waste? *J. Sci. Food Agric.* **2014**, *94*, 2357−2361.
(2) Clendennen, S. K.; May, G. D. Differential gene expression in ripening banana fruit. *Plant Physiol.* **1997**, *115*, 463−469.
(3) Klee, H. J. Control of ethylene-mediated processes in tomato at the level of receptors. *J. Exp. Bot.* **2002**, *53*, 2057−2063.
(4) Barry, C. S.; Giovannoni, J. J. Ethylene and fruit ripening. *J. Plant Growth Regul.* **2007**, *26*, 143−159.
(5) Lin, Z.; Zhong, S.; Grierson, D. Recent advances in ethylene research. *J. Exp. Bot.* **2009**, *60*, 3311−3336.
(6) Zhu, X.; Shen, L.; Fu, D.; Si, Z.; Wu, B.; Chen, W.; Li, X. Effects of the combination treatment of 1-MCP and ethylene on the ripening of harvested banana fruit. *Postharvest Biol. Technol.* **2015**, *107*, 23−32.
(7) Porat, R.; Weiss, B.; Cohen, L.; Daus, A.; Goren, R.; Droby, S. Effects of ethylene and 1-methylcyclopropene on the postharvest qualities of 'Shamouti' oranges. *Postharvest Biol. Technol.* **1999**, *15*, 155−163.
(8) Jaiswal, P.; Jha, S. N.; Kaur, P. P.; Bhardwaj, R.; Singh, A. K.; Wadhawan, V. Prediction of textural attributes using color values of

DOI: 10.1021/acs.jafc.6b02072
J. Agric. Food Chem. 2016, 64, 5164−5170

banana (*Musa sapientum*) during ripening. *J. Food Sci. Technol.* **2014**, *51*, 1179−1184.
(9) Valérie Passo Tsamo, C.; Andre, C. M.; Ritter, C.; Tomekpe, K.; Ngoh Newilah, G.; Rogez, H.; Larondelle, Y. Characterization of *Musa* sp. fruits and plantain banana ripening stages according to their physicochemical attributes. *J. Agric. Food Chem.* **2014**, *62*, 8705−8715.
(10) Prasanna, V.; Prabha, T. N.; Tharanathan, R. N. Fruit ripening phenomena—An overview. *Crit. Rev. Food Sci. Nutr.* **2007**, *47*, 1−19.
(11) Lohani, S.; Trivedi, P. K.; Nath, P. Changes in activities of cell wall hydrolases during ethylene-induced ripening in banana: Effect of 1-MCP, ABA and IAA. *Postharvest Biol. Technol.* **2004**, *31*, 119−126.
(12) Kojima, K.; Sakurai, N.; Kuraishi, S.; Yamamoto, R.; Inaba, A. Physical measurement of firmness of banana fruit pulp: Determination of optimum conditions for measurement. *Postharvest Biol. Technol.* **1992**, *2*, 41−49.
(13) Padmini, S.; Prabha, T. N. Biochemical changes during acetylene-induced ripening in mangoes (var. Alphonso). *Trop. Agric.* **1997**, *74*, 265−271.
(14) Hakim, M.; Obidul Huq, A.; Alam, M.; Khatib, A.; Saha, B.; Formuzul Haque, K.; Zaidul, I. Role of health hazardous ethephone on nutritive values of selected pineapple, banana and tomato. *J. Food, Agric. Environ.* **2012**, *10*, 247−251.
(15) Ban, T.; Kugishima, M.; Ogata, T.; Shiozaki, S.; Horiuchi, S.; Ueda, H. Effect of ethephon (2-chloroethylphosphonic acid) on the fruit ripening characters of rabbiteye blueberry. *Sci. Hortic.* **2007**, *112*, 278−281.
(16) Rizzuti, A.; Aguilera-Sáez, L. M.; Gallo, V.; Cafagna, I.; Mastrorilli, P.; Latronico, M.; Pacifico, A.; Matarrese, A. M. S.; Ferrara, G. On the use of ethephon as abscising agent in cv. Crimson seedless table grape production: Combination of fruit detachment force, fruit drop and metabolomics. *Food Chem.* **2015**, *171*, 341−350.
(17) Ugare, B.; Banerjee, K.; Ramteke, S. D.; Pradhan, S.; Oulkar, D. P.; Utture, S. C.; Adsule, P. G. Dissipation kinetics of forchlorfenuron, 6-benzyl aminopurine, gibberellic acid and ethephon residues in table grapes (*Vitis vinifera*). *Food Chem.* **2013**, *141*, 4208−4214.
(18) Yahia, A.; Kevers, C.; Gaspar, T.; Chenieux, J. C.; Rideau, M.; Creche, J. Cytokinins and ethylene stimulate indole alkaloid accumulation in cell suspension cultures of *Catharanthus roseus* by two distinct mechanisms. *Plant Sci.* **1998**, *133*, 9−15.
(19) Dhall, R. K.; Singh, P. Effect of ethephon and ethylene gas on ripening and quality of tomato (*Solanum Lycopersicum* L.) during cold storage. *J. Nutr. Food Sci.* **2013**, *3*, 244.
(20) Al-Baghli, N. A.; Loughlin, K. F. Binary and ternary adsorption of methane, ethane, and ethylene on titanosilicate ETS-10 zeolite. *J. Chem. Eng. Data* **2006**, *51*, 248−254.
(21) Berlier, K.; Olivier, M. G.; Jadot, R. Adsorption of methane, ethane, and ethylene on zeolite. *J. Chem. Eng. Data* **1995**, *40*, 1206−1208.
(22) Cen, P. L. Adsorption uptake curves of ethylene on Cu(I)−NAY zeolite. *AIChE J.* **1990**, *36*, 789−793.
(23) Choudhary, V. R.; Mayadevi, S. Adsorption of methane, ethane, ethylene, and carbon dioxide on high silica pentasil zeolites and zeolite-like materials using gas chromatography pulse technique. *Sep. Sci. Technol.* **1993**, *28*, 2197−2209.
(24) Jang, S. B.; Jeong, M. S.; Kim, Y.; Seff, K. Crystal structures of the ethylene and acetylene sorption complexes of fully Ca^{2+}-exchanged zeolite X. *J. Phys. Chem. B* **1997**, *101*, 3091−3096.
(25) Sardabi, F.; Mohtadinia, J.; Shavakhi, F.; Jafari, A. A. The effects of 1-methylcyclopropen (1-MCP) and potassium permanganate coated zeolite nanoparticles on shelf life extension and quality loss of golden delicious apples. *J. Food Process. Preserv.* **2014**, *38*, 2176−2182.
(26) Hardie, S. M. L.; Garnett, M. H.; Fallick, A. E.; Rowland, A. P.; Ostle, N. J. Carbon dioxide capture using a zeolite molecular sieve sampling system for isotopic studies (^{13}C and ^{14}C) of respiration. *Radiocarbon* **2005**, *47*, 441−451.
(27) Li, H.; Eddaoudi, M.; O'Keeffe, M.; Yaghi, O. M. Design and synthesis of an exceptionally stable and highly porous metal−organic framework. *Nature* **1999**, *402*, 276−279.
(28) Carson, C. G.; Hardcastle, K.; Schwartz, J.; Liu, X.; Hoffmann, C.; Gerhardt, R. A.; Tannenbaum, R. Synthesis and structure characterization of copper terephthalate metal−organic frameworks. *Eur. J. Inorg. Chem.* **2009**, *2009*, 2338−2343.
(29) Clausen, H. F.; Poulsen, R. D.; Bond, A. D.; Chevallier, M. A. S.; Iversen, B. B. Solvothermal synthesis of new metal organic framework structures in the zinc−terephthalic acid−dimethyl formamide system. *J. Solid State Chem.* **2005**, *178*, 3342−3351.
(30) Zhang, B.; Wang, Q. Development of highly ordered nanofillers in zein nanocomposites for improved tensile and barrier properties. *J. Agric. Food Chem.* **2012**, *60*, 4162−4169.
(31) Kim, J. G.; Luo, Y.; Tao, Y. Effect of the sequential treatment of 1-methylcyclopropene and acidified sodium chlorite on microbial growth and quality of fresh-cut cilantro. *Postharvest Biol. Technol.* **2007**, *46*, 144−149.
(32) Meng, X.; Lee, K.; Kang, T.-Y.; Ko, S. An irreversible ripeness indicator to monitor the CO_2 concentration in the headspace of packaged kimchi during storage. *Food Sci. Biotechnol.* **2015**, *24*, 91−97.
(33) Finney, E. E.; Bengera, I.; Massie, D. R. An objective evaluation of changes in firmness of ripening bananas using a sonic technique. *J. Food Sci.* **1967**, *32*, 642−646.
(34) Flitsanov, U.; Mizrach, A.; Liberzon, A.; Akerman, M.; Zauberman, G. Measurement of avocado softening at various temperatures using ultrasound. *Postharvest Biol. Technol.* **2000**, *20*, 279−286.

DOI: 10.1021/acs.jafc.6b02072
J. Agric. Food Chem. 2016, 64, 5164−5170